

Segmented attenuation correction for myocardial SPECT

Yasuyuki TAKAHASHI,* Kenya MURASE,* Teruhito MOCHIZUKI,** Hiroshi HIGASHINO,***
Yoshifumi SUGAWARA** and Akiyoshi KINDA****

*Department of Medical Engineering, Division of Allied Health Sciences, Osaka University Graduate School of Medicine

**Department of Radiology, Ehime University School of Medicine

***Department of Radiology, Ehime Prefectural Imabari Hospital

****Toshiba Medical Systems Engineering Laboratory

Purpose: One of the main factors contributing to the accuracy of attenuation correction for SPECT imaging using transmission computed tomography (TCT) with an external gamma-ray source is the radionuclide count. To reduce deterioration of TCT images due to inadequate radionuclide counts, a correction method, segmented attenuation correction (SAC), in which TCT data are transformed into several components (segments) such as water, lungs and spine, providing a satisfactory attenuation correction map with less counts, has been developed. The purpose of this study was to examine the usefulness of SAC for myocardial SPECT with attenuation correction. **Methods:** A myocardial phantom filled with Tc-99m was scanned with a triple headed SPECT system, equipped with one cardiac fan beam collimator for TCT and two parallel hole collimators for ECT. As an external gamma-ray source for TCT, 740 MBq of Tc-99m was also used. Since Tc-99m was also used for ECT, the TCT and ECT data were acquired separately. To make radionuclide counts, the TCT data were acquired in the sequential repetition mode, in which a 3-min-rotation was repeated 7 times followed by a 10-min-rotation 4 times (a total of 61 minutes). The TCT data were reconstructed by adding some of these rotations to make TCT maps with various radionuclide counts. Three types of SAC were used: (a) 1-segment SAC in which the body structure was regarded as water, (b) 2-segment SAC, in which the body structure was regarded as water and lungs, and (c) 3-segment SAC, in which the body structure was regarded as water, lungs and spine. We compared corrected images obtained with non-segmentation methods, and with 1- to 3-segment SACs. We also investigated the influence of radionuclide counts of TCT (3, 6, 9, 12, 15, 18, 21, 31, 41, 51, 61 min acquisition) on the accuracy of the attenuation correction. **Results:** Either 1-segment or 2-segment SAC was sufficient to correct the attenuation. When non-segmentation TCT attenuation methods were used, rotations of at least 31 minutes were required to obtain sufficiently large counts for TCT. When the 3-segment SAC was used, the minimal acquisition time for a satisfactory TCT map was 7 min. **Conclusion:** The 3-segment SAC was effective for attenuation correction, requiring fewer counts (about 1/5 of the value for non-segmentation TCT), or less radiation for TCT.

Key words: transmission computed tomography, emission computed tomography, segmented attenuation correction, myocardial SPECT

INTRODUCTION

SINCE THE PHOTON ENERGY of isotopes used for myocardial emission computed tomography (ECT) is relatively low, an accurate correction of intracorporeal attenuation is required. Attenuation correction using transmission computed tomography (TCT) with an external γ -ray source of ^{153}Gd or $^{99\text{m}}\text{Tc}$ has been reported to improve ECT

Received April 3, 2003, revision accepted December 17, 2003.

For reprint contact: Yasuyuki Takahashi, Ph.D., Department of Health, Health Planning Division, Ehime Prefectural Matsuyama Regional Office, 132, Kita-Mochida, Matsuyama, Ehime 790–8502, JAPAN.

E-mail: takahashi-yasuyuki@pref.ehime.jp

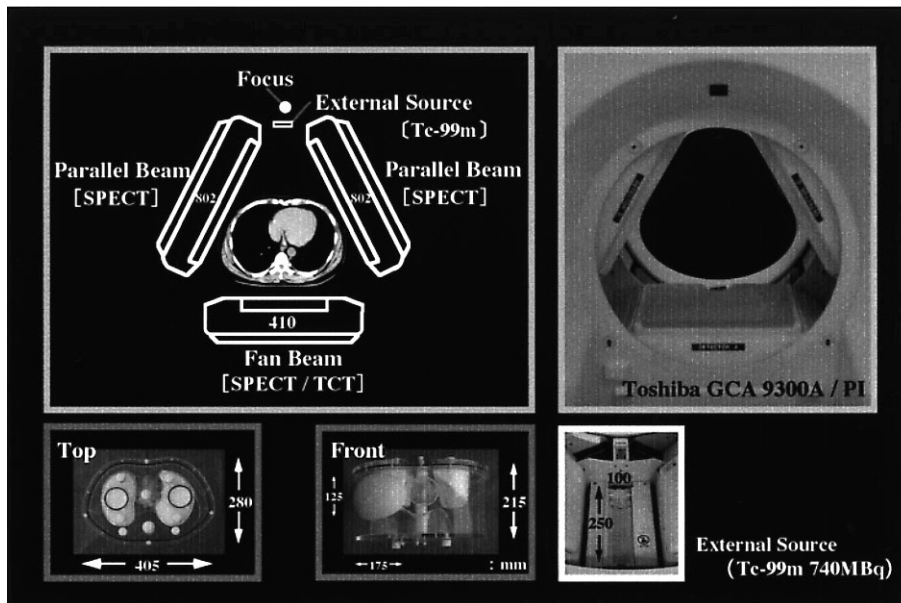


Fig. 1 The triple headed SPECT system and myocardial phantom used for TCT and ECT acquisition. The Sheet-like shape of the external γ -ray source, which was made from a bellows tube filled with 740 MBq of ^{99m}Tc , was placed at the focus of the fan beam collimator for TCT.

quantification.¹ However, the accuracy of correction using TCT images would be affected by the counts of TCT data.² It has been reported that an acquisition time of 15–20 min was required to obtain optimal TCT images from an external ^{99m}Tc source (1 GBq) using a gamma camera with 2 detectors.³ Data acquisition in a shorter period of time is desirable for reducing radiation exposure and the length of restraint during examinations.

Recently, segmented attenuation correction (SAC) has been used in positron emission tomography (PET). With this method, TCT data are transformed into data maps with several segments such as air, lungs, and soft tissue. Detailed TCT data are unnecessary, and so the data acquisition time is reduced.^{2–5}

In a clinical setting, an accurate attenuation-corrected myocardial image is essential for differentiating non-ischemic myocardium (uniform radionuclide counts) from ischemic myocardium (reduced radionuclide counts). In this study, we evaluated the usefulness of TCT with SAC in attenuation corrected myocardial SPECT, by examining various acquisition conditions for the SAC.

MATERIALS AND METHODS

SPECT system

The SPECT system used was a GCA-9300A/UI (Toshiba Medical Systems, Tochigi, Japan) equipped with one cardiac fan beam collimator and two parallel beam collimators. TCT data were acquired using an external gamma-ray source while myocardial ECT data were acquired using phantoms and a human subject (Fig. 1). The TCT external radiation source was a sheet-shape made from

bellows tube filled with 740 MBq of ^{99m}Tc . The tube, 1 mm in inner diameter, was made of a fluorocarbon resin embedded in an acrylic rectangular board of 30 cm \times 10 cm.⁶ The data processor was GMS-5500A/DI (Toshiba Medical Systems, Tochigi, Japan). Both TCT and ECT images were acquired with a matrix size of 128 \times 128, and a step and shoot mode (30 sec/direction) at intervals of 6 degrees (60 directions, 360-degree acquisition in total). Pixel size was 3.2 mm. Under these conditions, TCT projection counts/pixel were about 75 in the myocardial phantom and patients' myocardial area, and higher than 120 in the blank area. According to the triple-energy window (TEW) method,^{7,8} the acquisition window width was set at 20% of the main window (140 keV) with a subwindow of 7%.

Fan beam TCT data were transformed to parallel beam data. Any truncation in the transformed parallel beam data was corrected using non-truncated parallel beam data.⁹ An attenuation map was generated using filtered back projection (FBP). A ramp filter was used as a reconstruction filter. Butterworth filtering (cutoff = 0.31 cycle/cm, power factor = 8) was used as a post-reconstruction filter to decrease high frequency noise. ECT data of two parallel hole collimators were summed, followed by a 15 \times 15-point smoothing, then reconstructed using ordered subset-expectation maximization (OSEM: Number of iterations: 10, Subsets 5)⁶ with TEW scattering correction.

Description of the SAC algorithm

Three methods of segmentation were applied; SAC-1 in which the entire body outline of the myocardial phantom was regarded as water (a single peak), SAC-2, in which

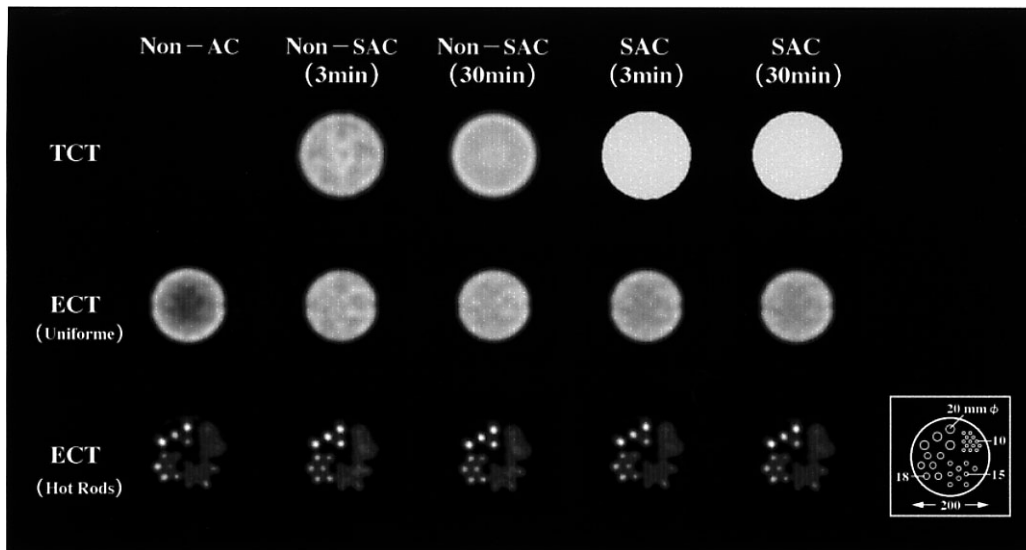


Fig. 2 The upper panel shows the attenuation image of the cylinder phantom, the middle panel the ECT image of the uniform phantom, and the lower panel the ECT image of the hot rods phantom. Images are uncorrected (Non-AC), corrected with the original TCT (Non-SAC) image (3 min or 30 min), or corrected with the SAC image (3 min or 30 min). A schema of the hot rods phantom is shown in the lower right.

the body outline was regarded as consisting of 2 peaks discriminating water and lung, and SAC-3, in which the body outline was regarded as consisting of 3 peaks discriminating water, lung and spine. A value for each segment was determined by linear transformation of coefficients of TCT map radiation attenuation using a fixed value,^{3-5,10} the coefficient being 0.028/cm in lung, 0.095/cm in water, and 0.107/cm in spine.

Phantom study

The TCT data were acquired using the sequential repetition mode, in which a 3-min-rotation was repeated 7 times followed by a 10-min-rotation 4 times (a total of 61 minutes). Then, TCT-attenuation maps with various counts were generated. As a control, the best TCT-attenuation map with the highest count was produced by summing all data acquired over 61 min. ECT images were reconstructed using these TCT-attenuation maps. Approximately 100 counts/pixel were obtained from each direction in the 30-min ECT acquisition. ECT and TCT acquisition were performed in the sequential mode.^{11,12} To avoid misregistration between the first (ECT) and second (TCT) images, the phantom was kept in the same position over the weekend a waiting the decay of the ECT data.

Uniform and hot rods phantoms

A cylinder phantom (200 mm in height and 200 mm in diameter, AZ-660, Anzai-Sogyo, Tokyo, Japan) was filled with 740 MBq of ^{99m}Tc. Hot rod areas (hot rods phantom) were established as shown in Figure 2. ECT images of these uniform and hot rods phantoms were generated by

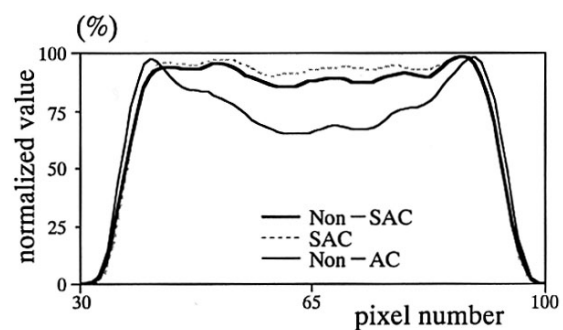


Fig. 3 Profile curves at the center of the uniform phantom. The TCT data were acquired over 30 min (Non-SAC, SAC and Non-AC).

non-SAC (3 min, 30 min) and SAC (3 min, 30 min). ECT images without attenuation correction were also compared. To evaluate the uniformity of the ECT images, we compared the profile curves generated by the non-SAC and the SAC (Fig. 3).

Myocardial phantom

In a myocardial phantom with a defect (20 × 20 mm) in the anterior wall (Data Spectrum Corp., Hillsborough, NC), the myocardial compartment was filled with 92.5 kBq/ml of ^{99m}Tc, and the thoracic region with 9.25 kBq/ml of ^{99m}Tc. ECT images and Bull's eye maps were generated using TCT images of SAC-1, -2, and -3 (Fig. 4). Those without attenuation correction were also generated.

ECT images and Bull's eye maps generated by non-SAC and SAC-3 (3 and 30 min) were compared (Fig. 5).

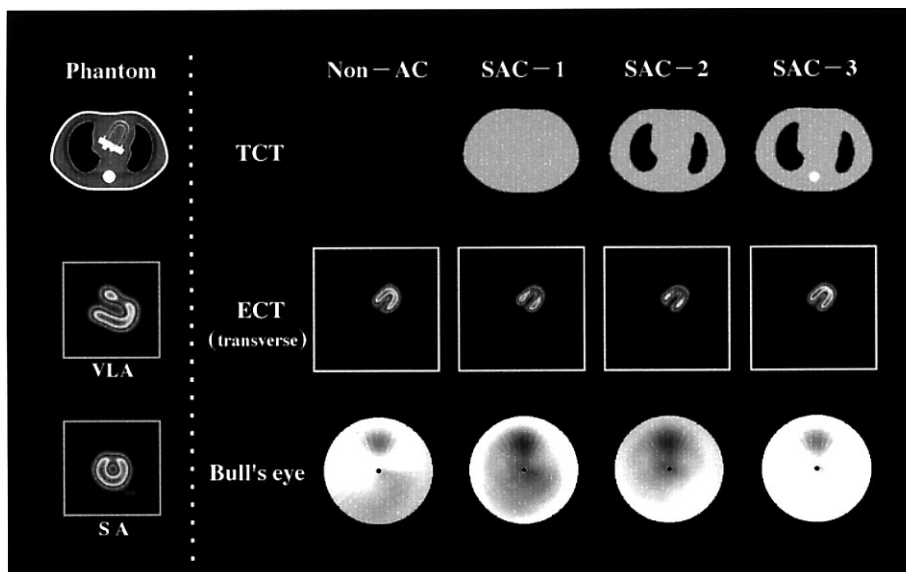


Fig. 4 Attenuation maps with each segment of the myocardial phantom (*upper row*), and SPECT images reconstructed using each map (*middle*) and the polar maps (*lower*). SAC-1 in which the entire body outline was regarded as water (a single peak). SAC-2, in which the entire body outline was regarded as consisting of 2 peaks corresponding to water and lungs. SAC-3, in which the body outline was regarded as consisting of 3 peaks corresponding to water, lungs and spine. The left side shows Non-AC. From top to bottom on the left, the myocardial phantom scheme (CT), and the myocardial images of the vertical long axis and short axis are shown. The CV of the Bull's eye maps corrected with SAC-1, -2, -3, was 24.24%, 13.92% and 3.09%, respectively. The CV without AC was 17.08%.

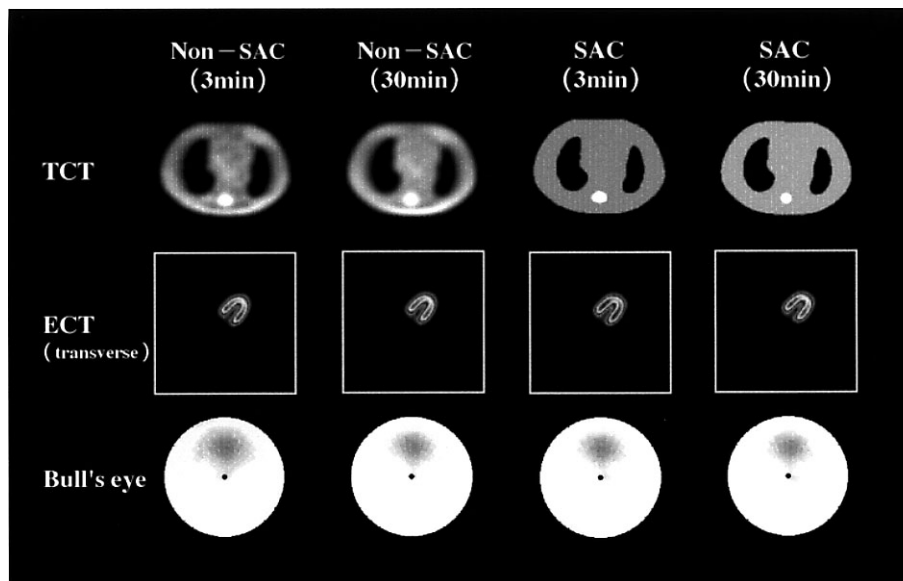


Fig. 5 The upper panel shows the attenuation maps (TCT images), the middle panel the SPECT images (ECT images), and the lower panel the polar maps (Bull's eye images) of the myocardial phantom. Images corrected with Non-SAC (3 min, 30 min) and SAC (3 min, 30 min) are shown from left to right for ECT and Bull's eye, respectively.

Human study

The human study was performed in a healthy 36-year-old male volunteer (Fig. 6). First, TCT was performed in the

sequential repetition mode like in the phantom experiments (over 45 min). Immediately after TCT, 740 MBq of ^{99m}Tc -tetrofosmin was injected intravenously. Ninety

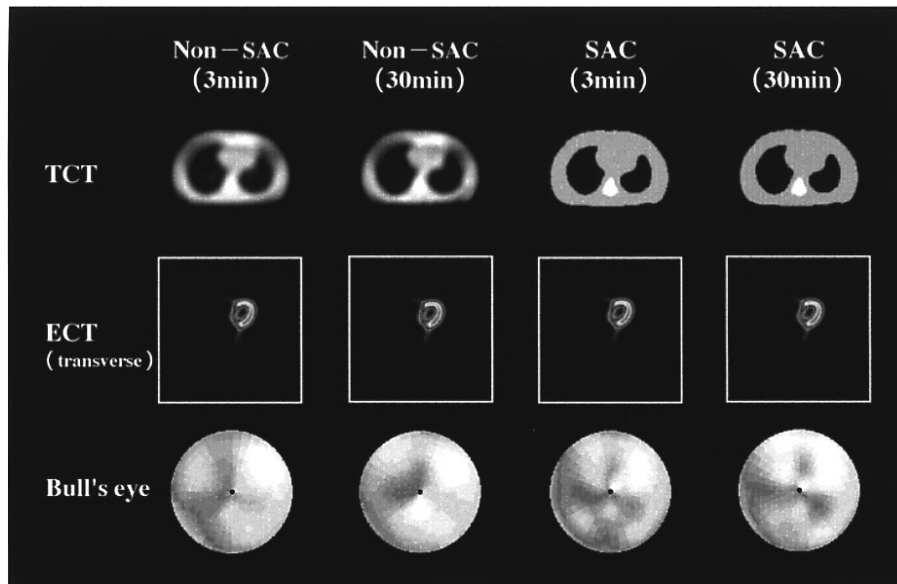


Fig. 6 The upper panel shows attenuation maps (TCT images), the middle panel SPECT images (ECT images), and the lower panel polar maps (Bull's eye images) of a human subject. Images corrected with Non-SAC (3 min, 30 min) and SAC (3 min, 30 min) are shown from left to right for ECT and Bull's eye, respectively.

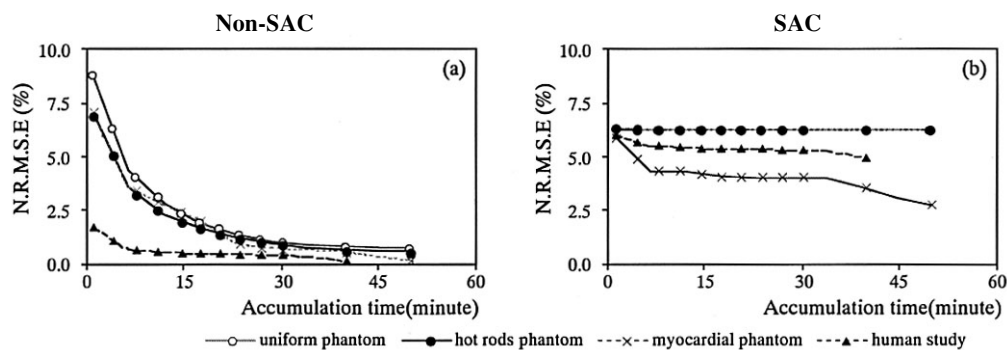


Fig. 7 Normalized root mean square errors (NRMSE) at each TCT acquisition time (Non-SAC, SAC) relative to the acquisition time for control data (61 min, Only the Human study is 41 min). (a) Non-SAC. (b) SAC.

minutes after the injection, ECT was acquired over 30 min (continuous mode). Four markers were placed on the body, and images were fused using the landmark method with an automatic registration tool (ART¹³). Images with TCT data acquired over various sampling times (3, 6, 9, 12, 15, 18, 21, 31 and 41 min) were created by summing some or all of the rotations. ECT images and Bull's eye maps generated by non-SAC and SAC-3 (3 min, 30 min) were compared (Fig. 6).

Evaluation

The uniformity in the ECT image of the cylinder phantom was expressed by a normalized mean value \pm standard deviation and coefficient of variance.

For a comparison of non-SAC and SAC over acquisi-

tion time, normalized root mean square errors [NRMSE (%)] were evaluated (Fig. 7). $[NRME (\%): \sqrt{[\sum(X_i - O_i)^2 / \sum O_i^2]} \times 100$: X_i : Measurement image, O_i : Standard image (non-SAC: 61 (41) min), i : pixel number ($i = 1 \sim n$)].¹⁴ In the evaluation of the uniform and hot rod phantoms, ECT images were used. In the myocardial phantom and human subject, Bull's eye maps were used.

RESULTS

Images and profile curves of the uniform and rods phantoms are shown in Figures 2 and 3. The normalized mean value (%) and CV (%) are 78.54 ± 15.60 and 19.86, respectively, in the images of the uniform phantom without attenuation correction (30 min). The normalized mean

value (%) and CV (%) are 92.33 ± 15.60 and 3.81 in the images of non-SAC TCT (30 min), and 95.96 ± 1.94 and 2.02 , in the images of SAC TCT (30 min). The NRMSE for the rods phantom was considered.

Images of the myocardial phantom (comparison among SAC-1, -2 and -3) are shown in Figure 4. The CV of the Bull's eye maps corrected with SAC-1, -2 and -3, was 24.24%, 13.92% and 3.09%, respectively. The CV without AC was 17.08%.

Images of the myocardial phantom (comparison between Non-SAC and SAC) are shown in Figure 5. The defect area established on the anterior wall differed significantly between Non-SAC TCT and SAC-3 TCT at 30 min.

Images of the human subject are shown in Figure 6. The same tendency was observed as in the myocardial phantom.

The NRMSE of Non-SAC and SAC over acquisition time are shown in Figure 7. When Non-SAC TCT was used, NRMSE reached a plateau at about 20 min for both the uniform and hot rods phantoms (Fig. 7a). When TCT with SAC was used, NRMSE reached a plateau at about 6 min (Fig. 7b). A plateau was attained at about 20 min with Non-SAC TCT and 9 min using TCT with SAC.

In the human study, time to plateau for a satisfactory image was 9 min with Non-SAC TCT (Fig. 7a) and 6 min for TCT with SAC-3 (Fig. 7b). As shown in Figures 5 and 6, the image obtained by Non-SAC TCT (3 min, 30 min) was equivalent to that obtained by TCT with SAC-3 (3 min, 30 min).

DISCUSSION

Attenuation correction by TCT with an external source^{1,11,15} or X-ray¹⁶ is currently available in SPECT imaging reconstruction. The use of X-rays has an advantage over the use of an external source in spatial resolution (and is less influenced by the partial volume effect), resulting in a more accurate AC-map. However, the accuracy of attenuation correction depends on the image registration between the AC-map and ECT data.¹⁷ Therefore, the AC-map generated using the X-ray CT method does not always guarantee accurate attenuation correction.¹⁸

On the other hand, substantial acquisition time (at least 15–20 min) is required to obtain optimal TCT images using an external source (^{99m}Tc of 1 GBq). Although data acquisition in a shorter time is desirable for clinical use, short-duration and count-limited TCT images have too much noise. Recently, PET studies have shown that segmented attenuation correction (SAC) is useful to reduce the acquisition time for TCT without increasing noise. Meikle et al.³ reported that using SAC, accurate attenuation correction was achieved with an acquisition time as low as 2 min without an increase in noise in reconstructed PET images. In this study, we evaluated

the feasibility of TCT with SAC both in phantom and in human cardiac SPECT.

We compared the uniformity of TCT images between the non-SAC and SAC methods. As shown in Figure 2, uniformity without SAC depended on the duration of the acquisition time and seemed to require approximately 20 min (i.e., the NRMSE reached a plateau at approximately 20 min, Fig. 7a) to obtain accurate and stable TCT images. On the other hand, the NRMSE remained constant in the ECT images obtained using SAC (Fig. 7b). The uniformity of ECT images using SAC was relatively independent of the data acquisition time. Indeed, visually there was little difference in either the SPECT or Bull's eye images, as shown in Figures 5 and 6. Thus, the shorter acquisition time achieved using SAC would reduce the dose or radiation to the patient.

As shown in Figure 4, the ECT images of the myocardial phantom corrected using the TCT image obtained with SAC-1 and SAC-2, were sub optimal when compared to the ECT images corrected with TCT using SAC-3. Similar results were previously reported in PET studies.

However, with SAC of a fixed value,^{3–5,10} depending on the number of segments, the value from which the present weak coefficient differs varies. Therefore, if one averages the count, there is a danger of affecting the attenuation value. From this study, although SAC-3 was of the same grade as Non-SAC (original) TCT and gave a comparatively good result, it is necessary to examine dividing a segment in detail further.

CONCLUSION

The 1-segment SAC and 2-segment SAC were insufficient for attenuation correction in human myocardial SPECT. The 3-segment SAC was effective for attenuation correction, requiring fewer counts (about 1/5 of the value for non-segmentation TCT) or less radiation dose.

ACKNOWLEDGMENTS

The authors thank Mr. Kenzo Ide, Mr. Shingo Izawa and Mr. Ryouyuke Ueda (Nihon Medi-Physics Co., Ltd.) for technical support.

REFERENCES

1. Van Laere K, Koole M, Kauppinen T, Monsieurs M, Bouwens L, Dierck R. Nonuniform transmission in brain SPECT using ²⁰¹Tl, ¹⁵³Gd, and ^{99m}Tc static line sources: Anthropomorphic dosimetry studies and influence on brain quantification. *J Nucl Med* 2000; 41: 2051–2062.
2. Meikle SR, Bailey DL, Hooper PK, Eberl S, Hutton BF, Jones WF, et al. Simultaneous emission and transmission measurements for attenuation correction in whole-body PET. *J Nucl Med* 1995; 36: 1680–1688.
3. Meikle SR, Dahlbom M, Cherry SR. Attenuation correction using count-limited transmission data in positron emission

- tomography. *J Nucl Med* 1993; 34: 143–150.
4. Xu M, Luk WK, Cutler PD, Digby WM. Local threshold for segmented attenuation correction of PET imaging of the thorax. *IEEE Trans Nucl Sci* 1994; 41: 1532–1537.
 5. Xu M, Cutler P, Luk WK. Adaptive segmented attenuation correction for whole-body PET imaging. *IEEE Trans Nucl Sci* 1996; 43: 331–336.
 6. Takahashi T, Murase K, Higashino H, Sogabe I, Sakamoto K. Receiver operating characteristic (ROC) analysis of image reconstructed with iterative expectation maximization algorithms. *Ann Nucl Med* 2001; 15: 521–525.
 7. Ogawa K. Simulation study of triple-energy-window scatter correction in combined Tl-201, Tc-99m SPECT. *Ann Nucl Med* 1995; 8: 277–281.
 8. Ichihara T, Motomura N, Ogawa K, Hasegawa H, Hashimoto J, Kubo A. Evaluation of SPET quantification of simultaneous emission and transmission imaging of the brain using a multidetector SPET system with the TEW scatter compensation method and fan-beam collimation. *Eur J Nucl Med* 1996; 23: 1292–1299.
 9. Motomura N, Ichihara T, Takayama T, Nishihara K, Inouye T, Kataoka T, et al. Practical method for reducing truncation artifacts in a fan beam transmission CT system. *J Nucl Med* 1998; 39: 178. (abstract)
 10. Takahashi Y, Higashino H, Sogabe I, Sakamoto K, Murase K, Motomura N. Segmented attenuation correction by phantom experiment. *KAKU IGAKU (Jpn J Nucl Med)* 2000; 5: 250. (abstract)
 11. Murase K, Tanada S, Inoue T, Sugawara Y, Hamamoto K. Improvement of brain single photon emission tomography (SPET) using transmission data acquisition in a four-head SPET scanner. *Eur J Nucl Med* 1993; 20: 32–38.
 12. Stone CD, McCormick JW, Gilland DR. Effect of registration errors between transmission and emission scans on a SPECT system using sequential scanning. *J Nucl Med* 1998; 39: 365–373.
 13. Ardekani BA, Braun M, Hutton BF, Kanno I, Iida H. A fully automatic multimodality image registration algorithm. *J Comput Assist Tomogr* 1995; 19: 615–623.
 14. Takahashi Y, Murase K, Higashino H, Mochizuki T, Motomura N. Attenuation correction of myocardial SPECT images with X-ray CT: Effects of registration errors between X-ray CT and SPECT. *Ann Nucl Med* 2002; 16: 431–435.
 15. Hashimoto J, Ogawa K, Kubo A, Ichihara T, Motomura N, Takayama T. Application of transmission scan-based attenuation compensation to scatter-corrected thallium-201 myocardial single-photon emission tomographic images. *Eur J Nucl Med* 1998; 25: 120–127.
 16. Bocher M, Balan A, Krausz Y, Shrem Y, Lonn A, Wilk M, et al. Gamma camera-mounted anatomical X-ray tomography: technology, system characteristics and first images. *Eur J Nucl Med* 2000; 27: 619–627.
 17. Murase K, Tanada S, Inoue T, et al. Effect of misalignment between transmission and emission scans on SPECT images. *J Nucl Med Technol* 1993; 21: 152–156.